Automaton model for the simulation of pedestrian flow implemented in a path-oriented coordinate system

Minjie Chen Günter Bärwolff Hartmut Schwandt

Institut für Mathematik, Technische Universität Berlin, Germany

minjie.chen@math.tu-berlin.de baerwolf@math.tu-berlin.de schwandt@math.tu-berlin.de

July 14, 2009

Abstract: Many discrete models for pedestrian flow simulation are based on cellular automata (CA). The geometry of these traditional models are generally defined on a two-dimensional regular grid. In the current paper, we present a new model for the simulation of pedestrian flow in which, instead of being regular, the underlying grid of the CA is constructed on a path-oriented coordinate system. The basic idea of our model is applicable for the grid-based methods of pedestrian flow simulation in general.

Keywords: cellular automaton, pedestrian flow, path-oriented coordinate system

1 Introduction

Over a decade computer simulation of pedestrian dynamics has been intensively investigated [5, 12, 6, 7, 10, 11, 14]. A major category of the modelling techniques is the microscopic simulation in which the pedestrians, also called *particle*s, are treated separately as individuals. In this category, cellular automata (CA) have proved to be an interesting tool to describe the particle behaviours [2, 8, 9]. Standard CA models are simple, but somewhat inflexible as they are mostly based on fixed time cycles, i. e. particles proceed with a constant speed, and as the fixed size of the usually quadratic, sometimes rectangular cells does not allow for a sophisticated simulation of real world scenarios. [3] introduced a microscopic model defined on a two-dimensional regular grid modelling individual particle velocities and considering the particle behaviours as a result of various induced impacts among them. At IMS 2008 [1] presented a simulation tool with virtually variable cell sizes.

[4] observed the behavioral characteristics of pedestrians on usual paths which need not to be straight and mentioned a so-called "path force" by which the particles are always pulled toward the centre line of the path. Despite the fact that a path, when not a straight line, can still be approximated on a two-dimensional regular grid without any technical difficulty, the potential moving directions expressed as a linear combination of the two unit vector of the axes of the grid and consequently, the position change of the particles, are often unrealistic. However, we may alternatively imagine such a path as an "orientation" dimension in a certain coordinate system which is sometimes called *path-oriented coordinate system*. The deviance from the centre line of the path serves as a natural second dimension. Equipped with this new definition, it is possible to describe this coordinate system as a curvilinear grid and consider the particle behaviours on it.

2 Model

The physical position in the path-oriented coordinate system of [4] is defined by its two components: the position on the centre line as a curve, and the deviation from this curve. Mathematically, the area representable in this coordinate system is the *tubular neighbourhood* of the path as a plane curve. In the sequel, we request this curve be regular, i. e. C^1-differentiable. (In fact, irregular points of a irregular curve may represent critical points on a path, such as crossings and junctions.)

AUTHORS' REMAKE IMS 2009 pp.925--932

2.1 Tubular neighbourhood

The original oriented path can be represented by a curve and, therefore, be described by a C^1-mapping $S : I \to \mathbb{R}^2$ from an interval $I \subset \mathbb{R}$ into $\mathbb{R}^2$, The deviation from the path can be measured by a number $r \in \mathbb{R}$, that is,

$$rN_S,$$

with N_S being the normal vector of the curve S. At a local position $S(t)$, $t \in I$ on the curve, the normal segment is defined by

$$N_{S,\delta}(t) = \{\, S(t) + rN_S(t) \mid r \in (-\delta, \delta) \,\},$$

for a given $\delta > 0$. In the application, we extend the neighbourhood to be a closed set to include the boundary, $r \in (-\delta, \delta)$ will be replaced by $r \in [-\delta, \delta]$. The tubular neighbourhood $N_{S,\delta}$ is defined as the union of disjoint normal segments of the curve, given by an injective mapping F on $S(I) \times (-\delta, \delta)$, that is,

$$\begin{aligned} F &: S(I) \times (-\delta, \delta) \to N_{S,\delta}(I), \\ F\left(S(I) \times (-\delta, \delta)\right) &= N_{S,\delta}(I) = \bigcup_{t \in I} N_{S,\delta}(t). \end{aligned} \tag{1}$$

The injectivity has to be guaranteed by the choice of a sufficiently small δ.

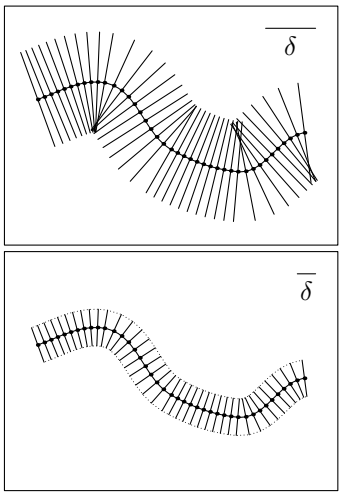

Figure 1: Above: Normal segments of an arbitrary curve with a too large δ. Below: Tubular neighbourhood of the same curve with a proper δ, F is in this case injective on $S(I) \times (-\delta, \delta)$ (cf. (1)).

2.2 Coordinate system

By $\mathcal{L}(\cdot)$ we denote the length of a curve. We require that a tubular neighbourhood of S can be defined with a proper choice of $\delta > 0$. Let $S_0 = S \circ \tau : [0, \mathcal{L}(S)] \to \mathbb{R}^2$ be the arc length parameterization of S. We further define

$$\begin{aligned} S_d &: [0, \mathcal{L}(S)] \to \mathbb{R}^2, \\ S_d(l) &= S_0(l) + dN_{S_0}(l) \end{aligned} \tag{2}$$

as the equidistant curve to S_0 with a deviation d in the range $[-\delta, \delta]$. N_{S_0} denotes the normal segment of S_0 at the local position parameterized by $l \in [0, \mathcal{L}(S)]$, that is, there holds

$$N_{S_0}(l) = N_S(\tau(l)) \quad \text{for all } l \in [0, \mathcal{L}(S)].$$

Apparently, given a tuple $(d, l) \in [-\delta, \delta] \times [0, \mathcal{L}(S)]$, a position in $\mathbb{R}^2$ is uniquely defined. By d and l we may build the *path-oriented* coordinate system. We give a simple example in Figure 2. In this coordinate system, a curvilinear grid can be constructed, in an analogous way to a rectangular grid on $\mathbb{R}^2$.

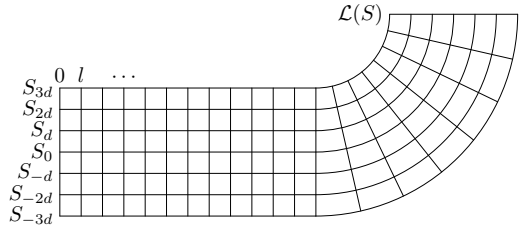

Figure 2: A simple example of the path-oriented coordinate system in two dimensions. In the first dimension (of d), a family of equidistant curves ($S_{jd}, j = 0, \pm 1, \pm 2, \pm 3$) are shown, the second dimension (of l) is measured by arc length.

2.3 Curvilinear grid

We consider a family of equidistant curves S_{jd}, for $j = 0, \ldots, \pm n$, $n \in \mathbb{N}^+$. Let $d > 0$ be known with the restriction that these curves are within a tubular neighbourhood of S. Consider the curve segment mapped from an interval $L = [l_a, l_b]$ ($0 \le l_a < l_b \le \mathcal{L}(S)$) by S_{jd}. We write this as S_{jd}^L.

From (2), the monotonicity of the lengths of the curve segments S_{jd}^L (for $j = -n, \ldots, 0, \ldots, n$) can be easily recognized. Without loss of generality, we assume

$$\mathcal{L}\big(S_{nd}^L\big) \le \cdots \le \mathcal{L}\big(S_0^L\big) \le \cdots \le \mathcal{L}\big(S_{-nd}^L\big), \tag{3}$$

i. e. monotonicity in the sense of Figure 2. To construct a curvilinear grid on the path-oriented coordinate system derived from S, we need a decomposition

$l_1, \ldots, l_{m-1}$ of the domain $[0, \mathcal{L}(S)]$ with

$$0 = l_0 < l_1 < \cdots < l_{m-1} < l_m = \mathcal{L}(S).$$

Starting from $l_0 = 0$, for every[1] interval $[l_{k-1}, l_k] = L_k \subset [0, \mathcal{L}(S)]$, $k = 1, \ldots, m$, we request l_k be chosen that

$$l_k := l_{k-1} + \Delta l,$$

with Δl satisfying

$$\mathcal{L}\left(S_{(n-1)d}^{[l_{k-1}, l_{k-1}+\Delta l]}\right) = d. \tag{4}$$

The repeated application of (4) yields a curvilinear grid composed of $2nm$ cells. For $j = 1, \ldots, n$ and $k = 1, \ldots, m$, the curvilinear grid cell bounded by $S_{(j-1)d}$ and S_{jd} between the arc length parameterization for l_{k-1} and l_k will be written as $c_{j,k}$; similarly, $c_{-j,k}$ stands for the cell bounded by $S_{-(j-1)d}$ and S_{-jd} between l_{k-1} and l_k.

(4) implies that the lengths and widths of the smallest cells are of the same magnitude. However, it is inevitable that some of the other cells may have large lengths. The size of these should be adjusted. Instead of the traditional curvature-based techniques, we suggest for the cell $c_{j,k}$ ($j = 1, \ldots, n$, $k = 1, \ldots, m$) the following

```
procedure refinement:
if ( L(S_jd^[l_{k-1}, l_k]) > α_k d )
then divide [l_{k-1}, l_k] into two equal sub-
  intervals and run procedure refinement
  on the resulting cells
return
```

to maintain that the cells are of approximately the same magnitude, i. e. size. We take into consideration a factor α_k of deformation of the inner cells $c_{n,k}$, for $k = 1, \ldots, m$,

$$\alpha_k = \frac{\mathcal{L}\left(S_{(n-1)d}^{L_k}\right)}{\mathcal{L}\left(S_{nd}^{L_k}\right)}, \tag{5}$$

measured by the side lengths. L_k denotes the relevant interval.

In an analogous way, for the cell $c_{-j,k}$ we check whether $\mathcal{L}\left(S_{-(j-1)d}^{[l_{k-1}, l_k]}\right)$ is larger than $\alpha_k d$. The main idea of the above procedure is to refine a curvilinear grid cell into two sub-cells, if both cell lengths on the l-axis are larger than $\alpha_k d$, the unit length adopted to define the family of equidistant curves (cf. (2)) multiplied by a deformation factor α_k (cf. (5)). If a monotonicity condition like (3) is known in the implementation, only the shorter length needs to be checked, as shown in the above pseudocode. For a simple example, we refer to Figure 3. The treatment of the reversed inequality ($\geq$) in (3) is obvious. A varying orientation of the curve can be treated by a subdivision into partial curves of unique orientation.

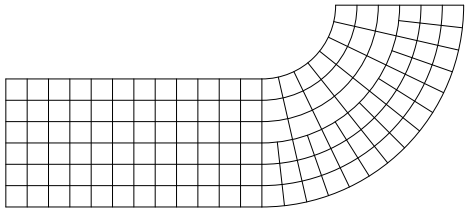

Figure 3: A simple example of the construction of curvilinear grid with refinement.

Technical note. On a regular two-dimensional grid, a grid cell (when not on the boundary) always possesses exactly one neighbour in all four directions (positive and negative in both dimensions). Due to this grid refinement procedure, this may not always be true on our refined curvilinear grid. For a sideward movement in the direction from the local centre of the curvature, sometimes two sub-cells serve as candidates. For a correct implementation, the selection of a proper neighbour among multiple possibilities (i. e. the two sub-cells), must be algorithmically specified. In the test case we implemented in § 3, a preference was given to the first sub-cells (in the positive direction of path orientation), when the step choice turned out to be impossible due to conflicts or other reasons, the second sub-cells would be investigated. In addition, this gives a physical interpretation that the particles are under the influence of a centrifugal force at the same time.

2.4 Step calculation on the grid

We may notice the fact that real human pedestrians are much more (when they are motivated toward some certain destination, that is, they possess a temporal moving direction) affected by the environmental settings in front of them than on the sides and behind them. In [3], an anisotropic variant of neighbourhood

1. This is the general case, it is possible that in the last step, (4) cannot be satisfied for an interval $[l_{m-1}, \mathcal{L}(S)]$. If the original path, i. e. S, is sufficiently long, $[l_{m-1}, \mathcal{L}(S)]$ can be divided and distributed evenly onto the other intervals.

n	$P(\rightarrow)$	$P(\uparrow)$, $P(\downarrow)$	$\sum P$
1	1	$1-D$	$3-2D$
2	$\frac{1}{2}+\frac{D}{2}$	$\frac{1}{2}-\frac{D}{2}$	$\frac{3}{2}-\frac{D}{2}$
3	$\frac{1}{3}+\frac{2D}{3}$	$\frac{1}{3}-\frac{D}{3}$	1
4	$\frac{1}{4}+\frac{3D}{4}$	$\frac{1}{4}-\frac{D}{4}$	$\frac{3}{4}+\frac{D}{4}$

Table 1: Probabilities for the step choices according to [8].

in elliptical shape has been suggested. The resulting prolongation matrix is unsymmetric, thus deserving future investigation in our model, with the matrix components (in terms of the its difference as a two dimensional index to the origin) closer (or aligning) to the current particle moving direction being given more weight. This unsymmetric prolongation matrix should be nontrivial. If we take a look at a waiting queue in the real world, in certain directions (i. e. on the sides) cell deactivation will be undertaken whereas the space is physically free, because people (in a well-formed context) choose to align with the queue direction.

On a two-dimensional regular grid, the simplest solution for a step calculation was suggested by [8], in which the particles took exactly one of the three step choices of going forward ($\rightarrow$), upward ($\uparrow$) or downward ($\downarrow$). The probabilities that a particle should take these choices were constructed according to the information collected in the neighbouring cells with the relative position $(\Delta x, \Delta y) \in \{(1,0),(-1,0),(0,1),(0,-1)\}$,

$$P(\rightarrow) = D + \frac{1-D}{n},$$
$$P(\uparrow) = P(\downarrow) = \frac{1-D}{n},$$

where n denotes the number of the unoccupied neighbouring cells, and $D \in [0,1]$ is a so-called drifting variable. This drifting variable D was assumed to be an empirical control variable under different geometric circumstances, so that the relative magnitudes of the probabilities in the three walking directions can be decided in accordance with the geometry in advance.

This implicitly requires a normalization in accordance with $\sum P$, cf. Table 1. We observe that a backstep is not allowed in this model. Additionally, the probability that a particle takes a stop as a step choice is implied to be 0; a particle takes a real stop in the simulation when denied any movement as the result of a conflict solution in the parallel update.

In our model, we consider the following three possible moving directions of the particles: one grid cell along the path, positive and negative deviation of one grid cell on the path. Although it can be considered as "one step forward", "one step to the left (or the right)" in a similar way as on a regular two-dimensional grid [8], we wish to point out that these step choices have a different meaning, in respect of the dimension, than those modelled in [8]. We associate the possible step choices with the probabilities P_l (along the path), P_d (with a positive deviation) and P_{-d} (with a negative deviation),

$$P_l + P_d + P_{-d} = 1, \qquad P_l, P_d, P_{-d} \geq 0.$$

Next, we distinguish two cases, that is, the particle flows along the current path free and at the same time subject to a so-called "path force" pulling it toward the centre of the path; or, the particle flows along the current path but is in the preparation of of direction change at a future point (e. g. a junction or a crossing the current path leads to).

In the first case, it can be assumed that the magnitude of the path force is proportional to the distance toward the centre line of the path. Applying the grid notation from § 2.3, the maximum of the possible deviation on the path is $\left(n-\frac{1}{2}\right)d$. For $j=1,\ldots,n$ and $k=1,\ldots,m$, the average distance of the grid cell $c_{j,k}$ toward the centre line is $\left(j-\frac{1}{2}\right)d$; the same holds for the grid cell $c_{-j,k}$ on the side of the centre line. It is reasonable therefore to give the step choice probabilities for a particle with a current position in grid cell $c_{j,k}$ (i. e. positively deviated)

$$P_l = 1 - P_{-d}, \tag{6a}$$
$$P_d = 0, \tag{6b}$$
$$P_{-d} = \frac{a}{a+1}, \qquad \text{with } a = \frac{j-\frac{1}{2}}{n-\frac{1}{2}}. \tag{6c}$$

Analogously, for a particle in a negatively deviated grid cell $c_{-j,k}$, there is $P_l = 1 - P_d$, and P_d, P_{-d} should interchange.

For the second case, we consider the following scenario: to be able to reach a crossing or a junction lying ahead of the current path (sometimes a future direction change will be involved as well), a particle must cover a certain distance Δd in the second dimension (i. e. the deviation) before progressing to a definite position with difference Δl ($\Delta l \geq 0$) in the first dimen-

sion (i. e. the path),

$$P_l = 1 - P_{\mathrm{sgn}\,(\Delta d)\,d}, \tag{7a}$$

$$P_{-\mathrm{sgn}\,(\Delta d)\,d} = 0, \tag{7b}$$

$$P_{\mathrm{sgn}\,(\Delta d)\,d} = \begin{cases} \frac{a}{a+1}, & \text{with } a = \frac{|\Delta d|}{\Delta l}, \quad \text{if } \Delta l \neq 0, \\ 1, & \text{if } \Delta l = 0. \end{cases} \tag{7c}$$

We explain this by a simple example illustrated in Figure 4. Consider a junction in the form of two

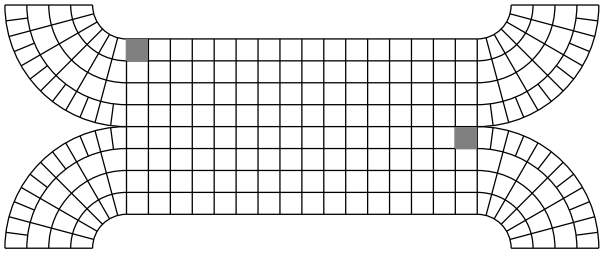

Figure 4: Example of a planned mandatory direction change: $\Delta l = 15$, $\Delta d = -4$.

paths linked together. All particles flow from left to right. A particle currently in the left gray cell $c_{4,1}$ aims to leave the junction through the second exit (next to the right gray cell $c_{-1,16}$). To ensure a successful direction change, when this particle reaches a position $l > 15$, (in the same column as the right gray cell $c_{-1,16}$, the second component of its position must be equal or less than -1. This yields[2] $\Delta l = 15$, $\Delta d = -4$ and (7a)–(7c) can be thus applied. Since the particle is under dominating influence toward a specific temporary destination position, we may assume that the path force effect (6a)–(6c) can be neglected here.

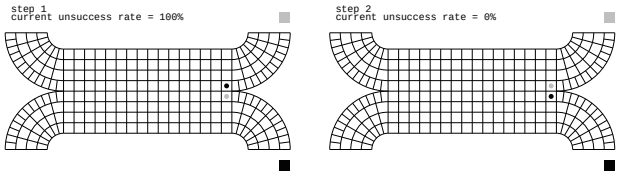

Figure 5: An simple example illustrating the solution of a critical conflict.

Technical note. A closer look at Figure 4 reveals that there exists a possibility not to be neglected of critical conflicts among the particles. Assume that a particle (shown as a black circle in Figure 5), positioned in grid cell $c_{1,16}$, is heading for the exit shown in black and another particle (shown in gray), positioned in grid cell $c_{-1,16}$, is heading for the other exit (in gray), as on the left of Figure 5. The two particles, due to their different ideal moving directions, develop into a "deadlock", blocking any possible further movement. Since real pedestrians, when encountering such a situation, would exchange their physical positions with each other (however in an awkward way), we may swap the particles' positions as a solution for the conflict, cf. the figure on the right. It becomes possible for the particles to move along their ideal paths. In the next section, we will see the difference of with and without this strategy.

The construction of (7a)–(7c) yields a planned walk over the shortest distance topologically from a position to another, i. e. in the relevant Euclidean coordinate system built by l and d. Consider an initial position (x_i, y_i) and and end position (x_e, y_e) and let $x_e > x_i$, $y_e > y_i$, without loss of generality. Let (x, y) be the current position. At this position, $a = \frac{y_e - y}{x_e - x}$, the expectation for a step choice in the y-direction is $\frac{a}{a+1}$, and in the x-direction, $\frac{1}{a+1}$. Interpreting these expectations as "forces" influencing the direction, the step choice fulfills

$$\frac{\mathrm{d}y}{\mathrm{d}x} = \frac{\frac{a}{a+1}}{\frac{1}{a+1}} = a = \frac{y_e - y}{x_e - x}$$

in the limit, i. e. for $\Delta \to 0$. The solution of this initial value problem is a straight line segment, i. e. the shortest connection joining (x, y) and (x_e, y_e).

3 Test Case Investigation

In this section, we give an implementation of a concrete test case. We consider the following common scenario: two paths join together in a certain region and then diverge again, particle movements are conducted on both of these two paths.

The particles start from the entrances "top-left" (abbreviated: "TL") and "bottom-left" (abbreviated: "BL") moving toward one of the exits "top-right" (abbreviated: "TR") and "bottom-right" (abbreviated:

2. The notation of the grid cells is established for good readability. Note there is no cell of the form $c_{0,k}$, so $\Delta d = -1 - 4 + 1 = -4$.

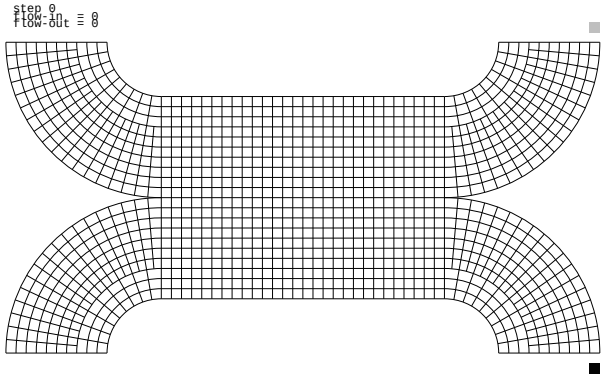

Figure 6: An simple example of curvilinear grid used in our test case implementation.

"BR"). The geometry of the model is given in Figure 6. Particles are produced on a random basis on the borders (in the negative dimension of the path orientation) of TL and BL.[3] They flow toward TR or BR and are drawn as small circles in different colours to indicate their ideal destinations. For the sake of simplicity, the centre lines of the four partial, curved paths TL, BL, TR and BR are defined as a $\frac{\pi}{2}$-arc each. In these regions the particles are subject to the path force. The rest of the area is understood as a central rectangle (abbreviated: "C").

The particle behaviours in the central region C deserve further investigation. We consider four possible situations. Some random tests have been protocolled in Figures 7 and 8.

In the simplest situation, the particles undergo no external influences, they merely flow forward, two main streams can be easily identified in the first part of Figure 7. In the second, the region C is considered as a part of the combined area of the two paths. Consequently, the particles are subjected to the path force in region C. In the second part of Figure 7 we see two streams merge into one and later separate again.

In the third situation, the particles are associated with a definite orientation in region C: they *must* flow toward their ideal destinations. The step choices were calculated by (7a)–(7c). Without any conflict solution, the central region C was characterized by high blockage percentage, cf. the first part of Figure 8. In the fourth situation, with the help of a critical conflict solution strategy (cf. the technical note in § 2.4), this problem had been much alleviated, see the second part of Figure 8.

In all the test cases, the produced particles (by a random probability in every simulation step) at the first column are counted as "flow-in" and those leave the last column as "flow-out". We can see that the four cases exhibit a similar flow-in number of the particles. The slightly higher value of test 1 is characterized by its nature of being practically free of collision. Cases 1 and 2 have further flow-out number in the same scale, the low flow-out number in case 3 shows the high occurrence of conflicts. In case 4, the conflict is partially solved and the result resembles real world situation roughly.

On the webpage `http://www.math.tu-berlin.de/~chenmin/misc/index.html` we provide four sets of full test results in PDF format and AVI format (encoded using the open source media player "MPlayer"[4]).

4 Further Discussion

In the current text, we discussed the construction of a curvilinear grid in dependence of a regular curve which further describes a walking path in the pedestrian dynamics. Since the curve orientation represents the main moving direction of the particles (pedestrians) on the path locally (i. e. between junctions and crossings, etc.), the current model may be used in combination with others or embedded in large grid-based simulation systems.

3. To be exact, the particles are introduced with an equal probability on the grid cells $c_{j,1}$ and $c_{-j,1}$ ($j = 1, \ldots, n$) and their possible sub-cells. They form a wide stream in the beginning and later this stream should tend to be condensed due to the path force, as can be seen from Figures 7 and 8.

4. `http://www.mplayerhq.hu`.

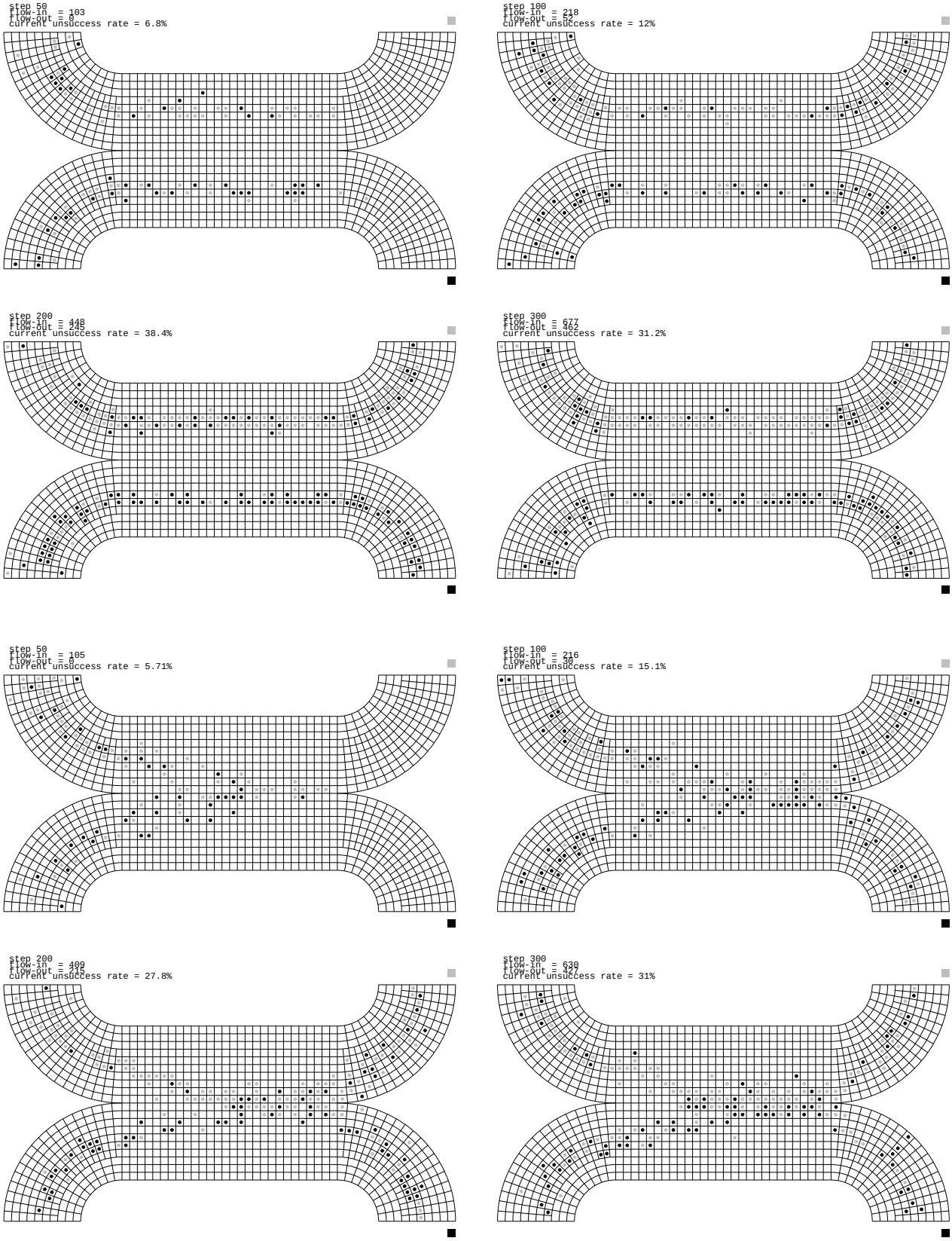

Figure 7: Test cases 1 and 2 after 50, 100, 200 and 300 simulation steps respectively.

AUTHORS' REMAKE IMS 2009 pp.925--932

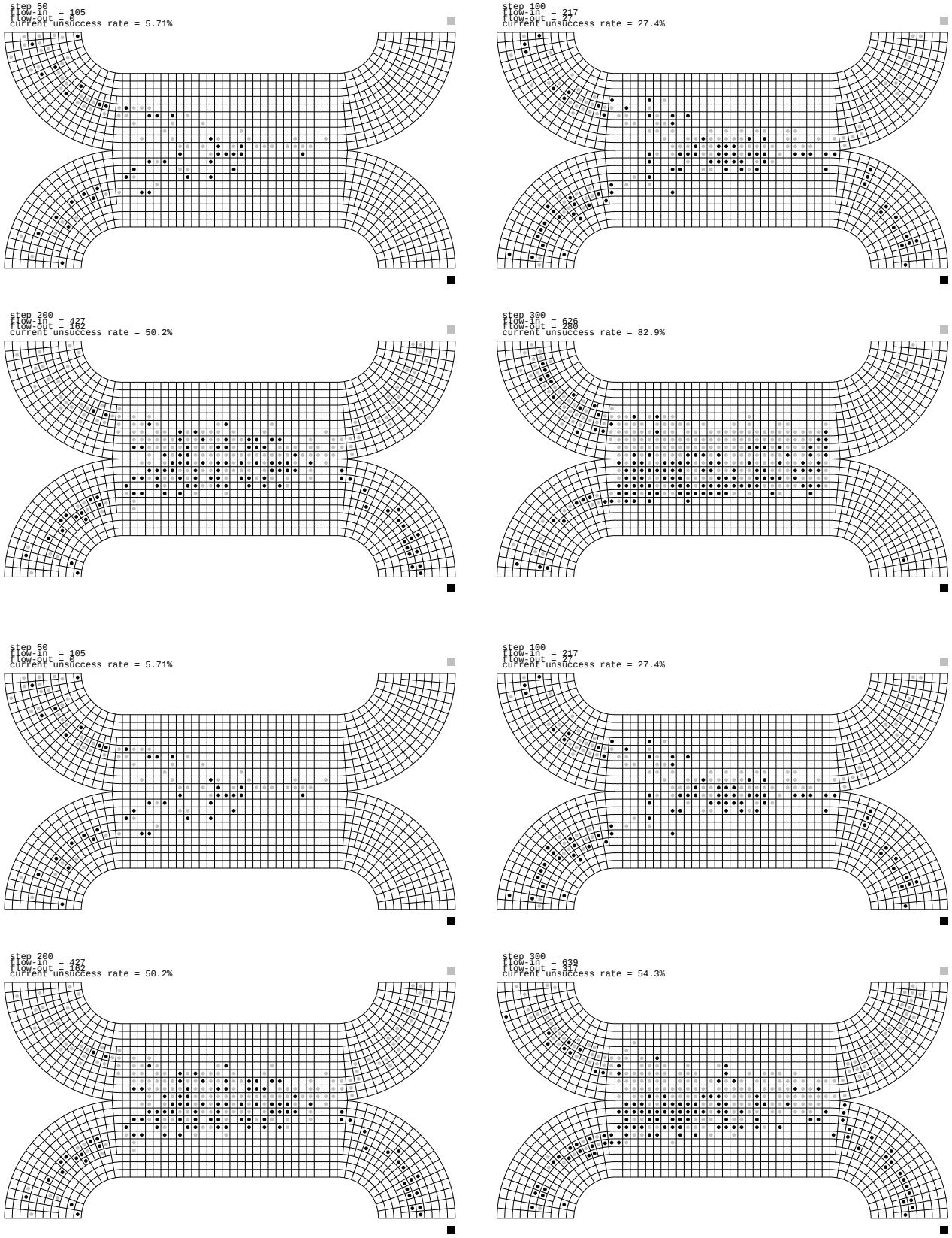

Figure 8: Test cases 3 and 4 after 50, 100, 200 and 300 simulation steps respectively.

AUTHORS' REMAKE IMS 2009 pp.925--932

References

[1] G. Bärwolff, M.-J. Chen, and H. Schwandt. Automaton model with variable cell size for the simulation of pedestrian flow. In E. Y. Li, editor, *Proceedings of the 7th International Conference on Information and Management Sciences 2008 (IMS 2008, 12–19 August 2008, Urumtschi, China)*, pages 727–736. California Polytechnic State University Press, Series of Information and Management Sciences, Vol. 7, Pomona, California, 2008.

[2] C. Burstedde, K. Klauck, A. Schadschneider, and J. Zittartz. Simulation of pedestrian dynamics using a two-dimensional cellular automaton. *Physica A*, 295:507–525, 2001.

[3] M.-J. Chen, G. Bärwolff, and H. Schwandt. A derived grid-based model for simulation of pedestrian flow. *J. Zhejiang Univ., Sci. A*, 10(2):209–220, 2009. doi: 10.1631/jzus.A0820049.

[4] C. Gloor, P. Stucki, and K. Nagel. Hybrid techniques for pedestrian simulations. In Sloot et al. [13], pages 581–590. ISBN 978-3-540-23596-5.

[5] D. Helbing. *Verkehrsdynamik: Neue physikalische Modellierungskonzepte*. Springer-Verlag Berlin Heidelberg, 1997. ISBN 3-540-61927-5.

[6] D. Helbing, H. J. Herrmann, M. Schreckenberg, and D. E. Wolf, editors. *Traffic and Granular Flow '99*. Springer-Verlag Berlin Heidelberg, 2000. ISBN 978-3-540-67091-9.

[7] S. P. Hoogendoorn, S. Luding, P. H. L. Bovy, M. Schreckenberg, and D. E.Wolf, editors. *Traffic and Granular Flow '03*. Springer-Verlag Berlin Heidelberg, 2005. ISBN 978-3-540-25814-8.

[8] A. Keßel, H. Klüpfel, J. Wahle, and M. Schreckenberg. *Microscopic simulation of pedestrian crowd motion*, pages 193–200. In Schreckenberg and Sharma [11], 2002. ISBN 978-3-540-42690-5.

[9] H. L. Klüpfel. *A cellular automaton model for crowd movement and egress simulation*. PhD thesis, Universität Duisburg-Essen, 2003.

[10] A. Schadschneider, T. Pöschel, R. Kühne, M. Schreckenberg, and D. E.Wolf, editors. *Traffic and Granular Flow '05*. Springer-Verlag Berlin Heidelberg, 2007. ISBN 978-3-540-47640-5.

[11] M. Schreckenberg and S. D. Sharma, editors. *Pedestrian and Evacuation Dynamics*. Springer-Verlag Berlin Heidelberg, 2002. ISBN 978-3-540-42690-5.

[12] M. Schreckenberg and D. E. Wolf, editors. *Traffic and Granular Flow '97*. Springer-Verlag Singapore, 1998. ISBN 978-981-3083-87-5.

[13] P. M. A. Sloot, B. Chopard, and A. G. Hoekstra, editors. *Proceedings of the 6th International Conference on Celluar Automata for Research and Industry, ACRI 2004*, volume 3305 of *Lecture Notes in Computer Science*, 2004. Springer-Verlag Berlin Heidelberg. ISBN 978-3-540-23596-5.

[14] N. Waldau, P. Gattermann, H. Knoflacher, and M. Schreckenberg, editors. *Pedestrian and Evacuation Dynamics 2005*. Springer-Verlag Berlin Heidelberg, 2007. ISBN 978-3-540-47062-5.

AUTHORS' REMAKE IMS 2009 pp.925--932